Subject-specificity of the correlation between large-scale structural and functional connectivity

[1]Zimmermann, J., [1]Griffiths, J., [2,3]Schirner, M., [2-6] Ritter, P., [1]McIntosh, A.R.

[1] *Baycrest Health Sciences, Rotman Research Institute, 3560 Bathurst St, Toronto, Ontario, M6A 2E1, Canada*

[2]*Charité – Universitätsmedizin Berlin, corporate member of Freie Universität Berlin, Humboldt-Universität zu Berlin, and Berlin Institute of Health, Dept. of Neurology*

[3]*Bernstein Focus State Dependencies of Learning & Bernstein Center for Computational Neuroscience, Berlin, Germany*

[4]*Minerva Research Group BrainModes, Max Planck Institute for Human Cognitive and Brain Sciences, Leipzig, Germany*

[5]*Berlin School of Mind and Brain & Mind and Brain Institute, Humboldt University, Berlin, Germany*

[6]*Berlin Institute of Health (BIH), Anna-Louisa-Karsch-Str 2, 10178 Berlin, Germany*

Abstract

Structural connectivity (SC), the physical pathways connecting regions in the brain, and functional connectivity (FC), the temporal co-activations, are known to be tightly linked. However, the nature of this relationship is still not understood. In the present study, we examined this relation more closely in six separate human neuroimaging datasets with different acquisition and preprocessing methods. We show that using simple linear associations, the relation between an individual's SC and FC is not subject-specific for five of the datasets. Subject-specificity of SC-FC fit is achieved only for one of the six datasets, the multi-modal Glasser HCP parcellated dataset. We show that subject-specificity of SC-FC correspondence is limited across datasets due to relatively small variability between subjects in the SC compared to the larger variability in FC.

Introduction

It has been shown that there is a relationship between structural connectivity (SC), the physical white-matter tracts between regions, and resting state functional connectivity (FC), the temporal coactivation between regions (Greicius, Supekar, Menon, & Dougherty, 2009; Hermundstad et al., 2013; Honey, Kotter, Breakspear, & Sporns, 2007; Honey et al., 2009; Koch, Norris, & Hund-Georgiadis, 2002; Misic et al., 2016; Ponce-Alvarez et al., 2015; Skudlarski et al., 2008; van den Heuvel, Mandl, Kahn, & Hulshoff Pol, 2009; van den Heuvel & Sporns, 2013) using both simple linear (Honey et al., 2009) as well as more complex metrics (Misic et al., 2016). Most of this research, however, considers group-averaged matrices of SC and FC rather than individual connectomes. Motivated by the recent interest in personalized medicine and precision science, there is a greater need to understand individual differences and unique relationships between SC and FC. One important question is whether individual SC correlates with the corresponding subject's FC to a greater extent than between-subjects. Correlations between whole-brain individual SC and FC have been associated with measures of behaviour or clinical conditions (Caeyenberghs, Leemans, Leunissen, Michiels, & Swinnen, 2013; Cocchi et al., 2014; Skudlarski et al., 2010; Zhang et al., 2011). Yet, there are very few studies that investigate the subject-specificity of this SC-FC correspondence (Honey et al., 2009; Meier et al., 2016), and as far as we know there are no studies that assert that individual SC maps best onto its corresponding FC using linear measures of association. One preliminary investigation conducted by Honey et al. (2009) examined this question, however results were inconclusive due to the limited sample. Clearly, it is not well understood whether there is a unique portion of variance in the SC accounting for unique individual differences in FC.

It has already been shown that individual structural and functional connectomes can be sensitive to age (Zimmermann et al., 2016), personality traits (Markett et al., 2013), or cognition, demographics and behaviour (Hearne, Mattingley, & Cocchi, 2016; Ponsoda et al., 2017; S. Smith, 2016; S. M. Smith et al., 2015), and that SC (Kumar, Desrosiers, Siddiqi, Colliot, & Toews, 2017; Munsell, 2017; Yeh et al., 2016) as well as FC (Enrico; Finn et al., 2015) can be used to identify individual connectome fingerprints, the extent of this individual variability has been called into question (Marrelec, Messe, Giron, & Rudrauf, 2016; Waller et al., 2017). This may particularly be the case in smaller sample sizes (Waller et al., 2017). It has been shown that variability in FC can be explained by only one or two dimensions, and that FC is highly degenerate in its ability to capture potential complexities and variability in underlying dynamics (Marrelec et al., 2016).

Variance decomposition methods, such as principal components analysis (PCA), are helpful for characterizing the strength of individual differences in connectomes (E. Amico, Goñi, J., 2017; Marrelec et al., 2016). PCA provides a simplified representation of the data by reducing the existing variance into a smaller number of components. In this way, the portion of variance that is common across subjects can be identified and separated from the unique aspects of the variance.

The aim of the present study is to investigate the subject-specificity of the SC-FC relationship. The analyses were conducted on several datasets with variable acquisition schemes and preprocessing methods on the findings: N1 = 48 (Ritter, Schirner, McIntosh, & Jirsa, 2013;

Zimmermann et al., 2016), N2 = 626 (Human Connectome Project, HCP), (Van Essen et al., 2013), N3 = 171 (Brown, Rudie, Bandrowski, Van Horn, & Bookheimer, 2012), N4 = 766 (HCP) with a high-resolution multi-modal parcellation (Glasser et al., 2016). Two additional datasets from the HCP were analyzed post-hoc. We use simple linear measures of association with bootstrapping to quantify the correspondence of within-subject and between-subject SC-FC, and decomposition to quantify the extent of common and unique variability in SC and FC across subjects.

Methods

Data acquisition and preprocessing

The analyses were conducted on 6 MRI datasets of healthy subjects: the Berlin dataset (N = 48) (Ritter et al., 2013; Schirner, Rothmeier, Jirsa, McIntosh, & Ritter, 2015; Zimmermann et al., 2016), the Nathan Kline Institute (NKI) Rockland dataset from the UMCD Multimodal connectivity database (N = 171) (Brown et al., 2012), and four variations from the Human Connectome Project (HCP) (S900 release) (Van Essen et al., 2013) which differed in terms of processing methods as well as parcellation schemes. The HCP Lausanne dataset (N = 626), and the HCP Glasser dataset (N = 766), the HCP Destrieux dataset (N = 754), and HCP Desikan-Killiany (DK) (N = 754). Note that sample size differences between HCP datasets are due to removal of subjects with problematic parcellations. The HCP Glasser dataset is a high-resolution multi-modal parcellation based on an areal feature-based cross-subjects alignment method (Glasser et al., 2016). Research was performed in compliance with the Code of Ethics of the World Medical Association (Declaration of Helsinki). Written informed consent was provided by all subjects with an understanding of the study prior to data collection, and was approved by the local ethics committee in accordance with the institutional guidelines at Charité Hospital, Berlin, UCLA, and HCP WU-Minn.

Table 1. Dataset details for 6 resting-state datasets, including sample size, preprocessing methods, and parcellation scheme.

	Berlin	NKI Rockland	HCP, Lausanne	HCP, Glasser	HCP, Destrieux	HCP, DK
Processing reference	Schirner et al. 2015	Brown et al. 2012	Glasser et al. 2013	Glasser et al. 2013	Glasser et al. 2013	Glasser et al. 2013

Number subjects	48	171	626	766	754	754
Subject ages	18-80 (M = 41.90, SD = 18.47)	5-85 (M = 35.80, SD = 19.99)	22-36 (M = 28.65, SD = 3.66)	22-37 (M = 28.78, SD = 3.70)	22-37 (M = 28.78, SD = 3.70)	22-37 (M = 28.78, SD = 3.70)
Structural and diffusion processing						
Software method	FreeSurfer (http://surfer.nmr.mgh.harvard.edu/)	FreeSurfer & Dipy	Diffusion Toolkit (http://trackvis.org/blog/tag/diffusion-toolkit/)	HCP pipeline (Glasser et al., 2013)	HCP pipeline (Glasser et al., 2013)	HCP pipeline (Glasser et al., 2013)
Motion & eddy-current correction	yes	yes	yes	yes	yes	yes
Intensity normalization	yes	no	yes	yes	yes	yes
Tractography	Probabilistic (MRTrix)	Deterministic (FACT)	Deterministic (EuDX)	Probabilistic (MRTrix)	Probabilistic (MRTrix)	Probabilistic (MRTrix)
SC Metric	Number of voxel pairs connected with streamline(s), regional volume corrected	Number of streamlines	Number of streamlines	Streamline count (SIFT2) weighted by inferred cross-sectional area of the streamlines	Weighted streamline count (SIFT2)	Weighted streamline count (SIFT2)
Functional processing						
Software method	Schirner et al 2015	fMRI FEAT	Glasser et al 2013	Glasser et al 2013	Glasser et al 2013	Glasser et al 2013
Slice-timing	no	yes	no	no	no	no
Motion correction	MCFLIRT	MCFLIRT	FIX denoising	6 DOF FLIRT, FIX denoising	6 DOF FLIRT, FIX denoising	6 DOF FLIRT, FIX denoising
Nuisance regression	yes (6 motion, mean WM, CSF)	Yes (24 motion, mean WM, CSF, mean whole brain)	no	no	no	no
Smoothing	no	yes (Gaussian	no	yes (Cortical	See Glasser	See Glasser

		kernel 5mm full-width half maximum)		within surface, subcortical volume smoothing, FWHM 2 mm Gaussian)	(column to the left)	(column to the left)
Intensity normalization of BOLD	no	yes	no	yes	yes	yes
Temporal filtering	High-pass filtering (cutoff at 100s)	Bandpass filtering (0.08-0.009Hz)	no	no	no	no
Registration to standard space	no	MNI152	no	MNI152 & surface-based areal feature multimodal registration (MSMAll, Robinson et al., 2014)		
Motion scrubbing	no	yes	no	no	no	no
Parcellation (total number of regions)	Desikan-Killiany (68) (Desikan et al., 2006)	Craddock (188)	Lausanne (83) (Hagmann et al., 2008)	Glasser (378) (Glasser et al., 2016), brainsem was removed	Destrieux (164) (Destrieux, Fischl, Dale, & Halgren, 2010)	Desikan-Killiany (84) (Desikan et al., 2006)

A detailed description of data acquisition procedures is presented in Table S1. Subject sample size, age range, post processing, and parcellation information are presented in Table 1, with links to previously published papers with these datasets. Quality control is described in detail there. Noise-correction was performed via nuisance variable regression from the BOLD signal, for the Berlin and Rockland dataset, including the 6 motion parameters, mean white matter, and CSF signals. For the HCP dataset, we used FIX-denoised data, a tool that was trained to effectively remove components of the white matter, CSF, physiological noise, and 24 high-pass filtered

motion parameters from the signal (Glasser et al., 2013). (See Table 1 for detailed information and references to data processing).

SC and FC was derived via diffusion-weighted magnetic resonance imaging (dwMRI) and resting-state blood oxygen dependent functional magnetic resonance imaging (rsfMRI BOLD) respectively. Structural and functional data were parcellated into predefined ROIs that varied in size across datasets (68-378 cortical regions). Fiber track estimation was performed on the diffusion data, and weight and distance SCs were computed by aggregating tractography-based estimations of white matter streamlines between regions of interest (ROIs). Each entry in the SC weights matrix estimates the connection strength between a pair of ROIs. SC distances were the Euclidian distances (Brown et al., 2012; Glasser et al., 2013; Hagmann et al., 2008), or average length of tracks (Schirner et al., 2015) in mm between pairs of ROIs. We corrected for SC distance by regressing distances from weight SCs, and using residuals for analysis (as tract length may have an effect on structure-function relations (Romero-Garcia, Atienza, & Cantero, 2014). To account for age-related differences in parcellation and ROI size, pair-wise SC (Berlin data set) connection weights were weighted by mean gray-matter white-matter interface area of connected ROIs. FCs were computed as the Pearson's correlation between each ROI pair of BOLD time series. We transformed FC matrix entries of each FC to become normally distributed by conducting a Fisher's r to Z transform.

Subject specificity of SC-FC predictions

We compared individual SC and FC within and between all subjects using Pearson's correlations, in order to determine whether individual SC correlates best with its own individual FC. We constructed a matrix of size N_{SC} x N_{FC} (N = the number of subjects $N_{SC} = N_{FC}$). The diagonal of this matrix captures the intra-subject (within) SC-FC correlations; the off-diagonal represent the inter-subject (between) SC-FC (See Figure 1 for a visualization of this SC-FC matrix). We corrected the p-value of each correlation value in the resulting matrix for multiple comparisons using FDR (Matlab function fdr_bky) (Benjamini, Krieger, & Yekutieli, 2006). Note that associations between all individual SC and FC within and between all subjects was also performed via eigenvector correlations. This method is described in the Supplementary Materials.

We conducted 1000 bootstrapped means of SC-ownFC correlations and 1000 boostrapped means of SC-otherFC correlations (Matlab function bootstrp) and plotted the two bootstrapped distributions against each other. In order to evaluate the statistical significance of the differences between the distributions, we subtracted the SC-otherFC distribution from the SC-selfFC distribution and constructed a 95% confidence interval on this difference distribution (Matlab function prctile). To confirm our results, in a secondary analysis we used only *SC present connections*, as indirect connections may have an unknown effect on FC (Honey et al., 2009). For this analysis, connections that have a zero value in the SC matrix were not included in the correlations with FC.

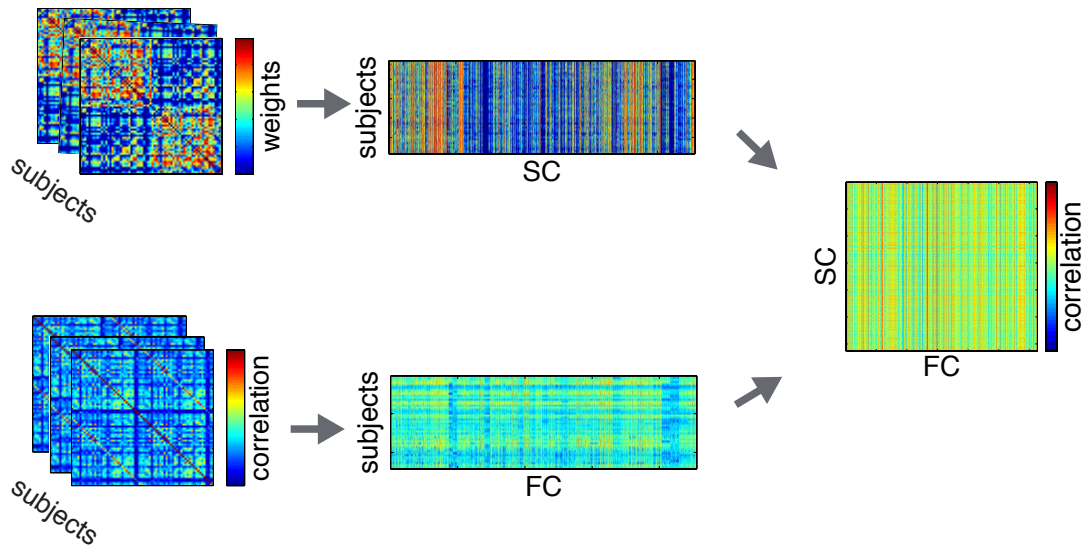

Figure 1. Individual subject SCs and FCs are stacked into a subjects x structural connections matrix and a subjects x functional connections matrix. Subject-wise SC and FC were then correlated for all pairs of SC and FC (within and between subjects). On-diagonals of this matrix are within subject SC-FC (SC-SelfFC), off-diagonals represent between subject SC-FC (SC-OtherFC).

Subject variability in SC and in FC

We examined variability across subjects in SC, as well as FC, in order to understand whether the lack of subject-specificity of SC-FC in the Berlin, HCP Lausanne and NKI Rockland dataset was due to a large portion of common variance in the connectomes across subjects that over-powered any existing individual differences. To this end, we decomposed the subject-wise SC matrix (SC connections x subjects) and FC matrix (FC connections x subjects) each with PCA (princomp function matlab, subjects as variables). The breakdown of variability in SC, as well as FC across subjects was thus ascertained. From the PCA, we obtained, for each PC: eigenvalues, the principal component loadings per subject, and principal component scores per each connection. To determine the significance of the resulting eigenvalues, we permuted the SC matrix and the FC matrix 100 times (scrambled across connections and subjects) and performed PCA of the resulting matrices to generate null distributions of eigenvalues for each PC. A p-value for each PC eigenvalue was obtained as the proportion of times that the permuted eigenvalue exceeded the obtained eigenvalue.

We also computed the age relationship with the principal component subject loadings that had been obtained from the PCA. We did this by calculating the correlation (via Partial Least Squares) of age (age vector, size: subjects x 1) with the subjects' principal coefficient loadings of the significant PCs (size: subjects x number of significant PCs). Partial Least Squares is a multivariate method akin to canonical correlation in that it computes the relationship between two matrices via orthogonal latent variables (Krishnan, Williams, McIntosh, & Abdi, 2011; McIntosh & Lobaugh, 2004). The significance of the resulting correlations was assessed via permutation testing (N = 1000) of the singular values from singular value decomposition of the

two matrices, and reliability of each principal component subject loading to the latent variable was assessed via bootstrapping (N = 500). We thus were able to compute how age corresponded to the significant variance across subjects.

Results

Subject specificity of SC-FC predictions

We first quantified the SC-FC relationship at the average group level. The correlation between averaged SC and averaged FC was as follows: Berlin: mean $r = 0.59$, HCP Lausanne: mean $r = 0.47$, NKI: mean $r = 0.41$, HCP Glasser: mean $r = 0.34$, HCP Destrieux: mean $r = 0.40$, HCP DK: mean $r = 0.47$, all $p < 0.001$.

At the individual subject level, all subjects' SCs were significantly correlated with all subjects' FCs (between and within SC-FC) (Pearson's correlations, $p < 0.001$, FDR multiple comparison correction, $p < 0.001$). However, we found that SC-FC correlations were subject-specific only for the HCP Glasser dataset, and not for the other datasets, when comparing the bootstrapped within-subject SC-FC correlation distribution (SC-SelfFC) and the bootstrapped between-subject SC-FC correlation distribution (SC-OtherFC) (CIs on difference distribution). The HCP Glasser dataset was the only dataset that showed subject-specificity using both the simple bivariate correlation (See Figure 2), as well as the eigenvector correlation approach (See Figure S2). Mean and CIs on the difference distributions are shown in Table 2 below for simple correlations and Table S2 for eigenvector correlations. The results were consistent using the two approaches.

Table 2. Mean and 95% CIs of the difference distribution calculated as the difference between the SC-SelfFC distribution and SC-OtherFC distribution. The * indicates a significant subject-specificity so that the distribution of intra-subject SC-FC is higher than the distribution of inter-subject SC-FC.

Dataset	**Simple correlation**	
	Mean	**CI**
Berlin	M = 0.0013	[-0.0169, 0.0190]
HCP, Lausanne	M = 0.0016	[-0.0012, 0.0044]
NKI Rockland	M = -5.8447e-04	[-0.0109, 0.0065]
HCP, Glasser	M = 0.0032	[0.002, 0.0043] *
HCP, Destrieux	M = -2.2348e-04	[-0.0019, 0.002]
HCP, DK	M = 0.001	[-.0001, 0.0017]

In summary, we found that for all but the HCP Glasser dataset, subject's SC did not correlate better with its own FC than with that of another subject's FC. These results remained consistent when using distance corrected SCs, or only SC present connections. For the HCP Glasser dataset, the within-subject SC-FC was significantly higher than the between-subject SC-FC when comparing the bootstrap resampled distributions.

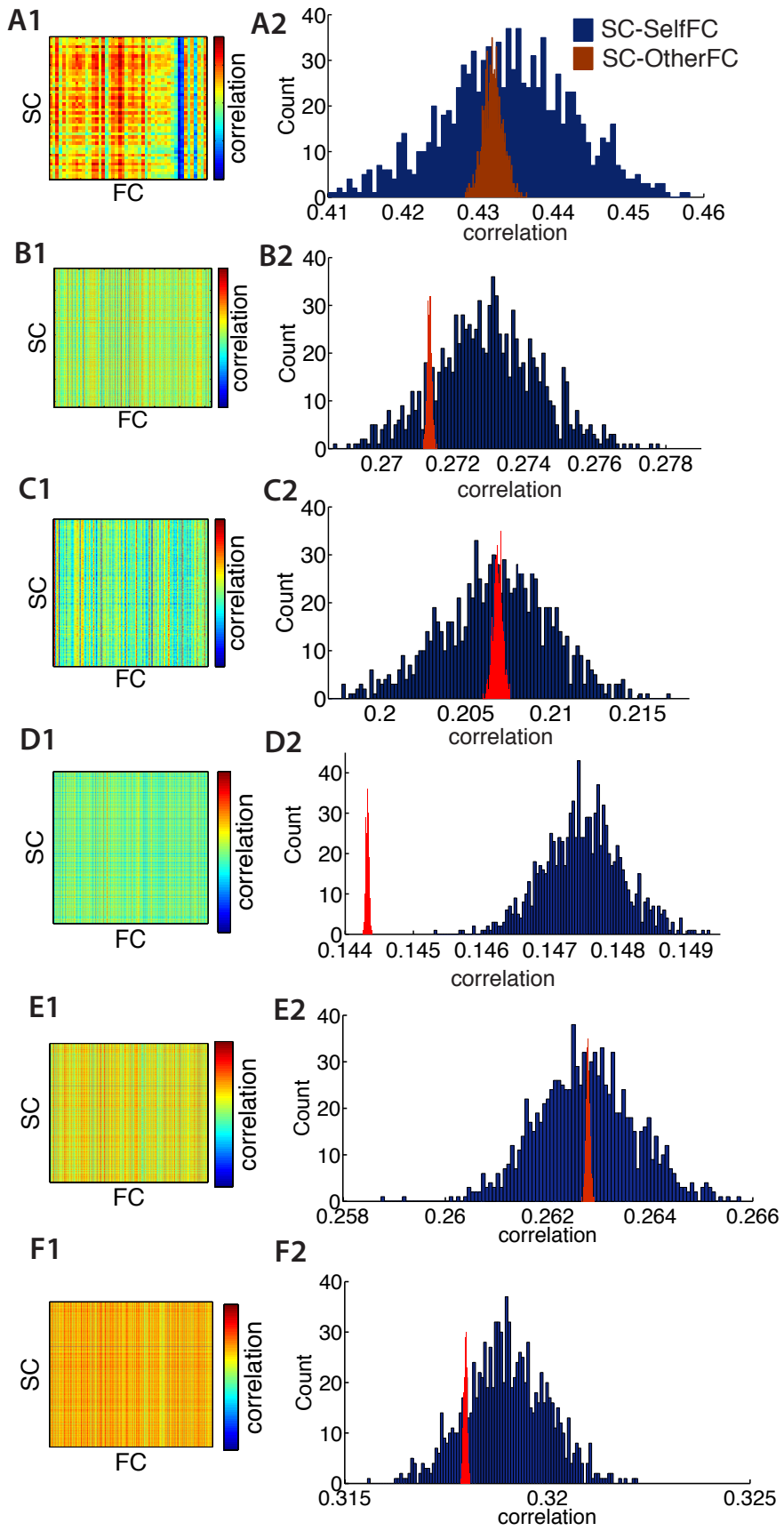
A1
SC
FC
correlation
A2
SC-SelfFC
SC-OtherFC
Count
correlation
B1
B2
C1
C2
D1
D2
E1
E2
F1
F2

Figure 2. Bivariate Pearson's correlations for all combinations of SC and FC within and between subjects, for **A1)** Berlin dataset **B1)** HCP Lausanne dataset **C1)** Rockland dataset **D1)** HCP Glasser dataset, **E1)** HCP Destrieux dataset **F1)** HCP DK dataset
and distribution histograms of bootstrapped means of intra (SC-SelfFC) and inter (SC-OtherFC) correlations for the **A2)** Berlin dataset **B2)** HCP Lausanne dataset and **C2)** Rockland dataset **D2)** HCP Glasser dataset **E2)** HCP Destrieux dataset **F2)** HCP DK dataset. SC-SelfFC correlations are those where SC and FC are from the same subject. SC-OtherFC correlations are those where SC and FC are from different subjects. Significance of the difference of these two distributions is calculated via CIs on the difference distribution.

Subject variability in SC and in FC

Figures 3 through 8 show PCA results for Berlin, HCP Lausanne, NKI, HCP Glasser, HCP Destrieux, and HCP DK data respectively. For both SC and FC across our datasets, the first component captured a very large portion of 'common' variance across subject. All subjects loaded heavily on this common PC1; these principal component subject loadings are visualized on the right-hand-side bar plots in Panel B in Figures 3-8. The principal component scores (ie., reconstructed matrix from PC1) for this common PC1 are visualized in the left-hand-side matrices in Figures 3-8. These represent the features of the connectome that were captured by PC1. The variance explained by this first 'common' PC was large in the SC (91%, 80%, 79%, 91%, 93% variance explained for Berlin, HCP Lausanne, NKI, HCP Glasser, HCP Destrieux, HCP DK datasets respectively) and lower in the FC (57%, 70%, 33%, 74%, 80% variance explained for Berlin, HCP Lausanne, NKI, HCP Glasser, HCP Destrieux, HCP DK data sets). Eigenvalues for the first 30 PCs for all datasets are shown in Supplementary Table S3.

A second pattern of results that we observed across all datasets was that SC was less variable than FC across subjects. There were fewer significant eigenvalues for the SC compared to the FC (significance determined via permutation testing of the eigenvalues), see Table S2 in the Supplementary Materials. From the figures (Panel A in Figures 3-8), the knee, or drop-off in the variance explained by subsequent PCs (Cattell, 1966) was evidently sharper for the SC than the FC. Thus although the common component was dominant for both modalities, the second and later components explained a larger portion of variance in the FC.

Consistent with the above findings, we also noted differences between SC and FC in the strength of the age-related differences. We found an age effect in the FC in all 6 datasets, (PLS analysis: Berlin: $r = 0.79$, $p < 0.001$, HCP Lausanne: $r = 0.42$, $p < 0.001$, NKI: $r = 0.63$, $p < 0.001$), HCP Glasser: $r = 0.43$, $p < 0.001$, HCP Destrieux: $r = 0.40$, $p < 0.001$, HCP DK: $r = 0.38$, $p < 0.001$ and in the SC for 2 of the 6 datasets (Berlin (non-significant): $r = 0.06$, $p = 0.68$, HCP Lausanne (non-significant): $r = 0.12$, $p = 0.48$, NKI (significant): $r = 0.50$, $p < 0.001$), HCP Glasser (significant): $r = 0.14$, $p = 0.035$), HCP Destrieux (non-significant): $r = 0.13$, $p = 0.13$, and HCP DK: $r = 0.13$, $p = 0.05$.

We compared brain volume across subjects to check for any age-related differences. For the Berlin and the Rockland dataset, tissue segmentation was performed and partial volume maps were derived using FSL FAST. Total brain volume was computed by summing the GM and WM tissue volumes. Total brain volume across subjects was correlated with region-wise SC (Berlin dataset: $r = 0.22$, $p = 0.14$, Rockland dataset: $r = 0.18$, $p = 0.17$) and FC (Berlin dataset: $r = 0.17$,

$p = 0.31$, Rockland dataset: $r = 0.09$, $p = 0.40$), no effect was found. Volume differences in the HCP data were already accounted for via the FIX method.

Finally, it is noteworthy that our results remained robust following a number of secondary analyses. For example, global signal regression and logarithm transformed SCs redistributed to a Gaussian distribution by resampling (Honey et al., 2009) to address the exponentially distributed connection weights. The results shown are those based on the original matrices. Please see Supplementary Table S2 for the PCA results on logarithmized SCs redistributed to Gaussian.

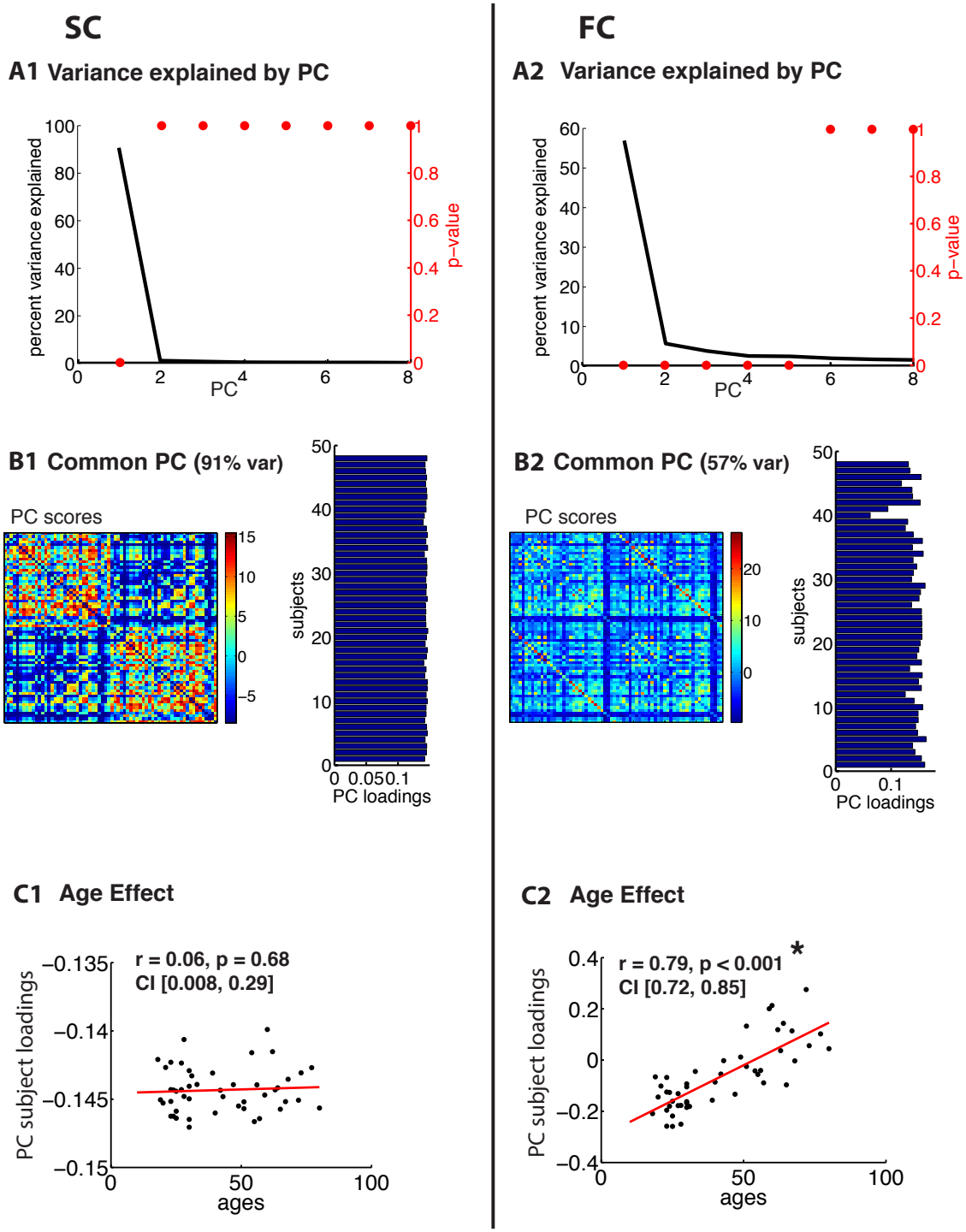

Figure 3. PCA of SC and FC matrices on Berlin data. Percent of total variance explained by each principal component of the **A1)** SC and **A2)** FC, with corresponding p-values. Panel B shows on the left-hand-side the principal component scores per connection for PC1, **B1)** for the

SC, and **B2)** for the FC. This shows the aspects of the connectome that are manifested in PC1, the common (across subjects) component. On the right-hand-side of panel B are the subject loadings onto PC1, all subjects load positively on this component. **C1)** shows the age effect for the SC and **C2)** shows the age effect for the FC..

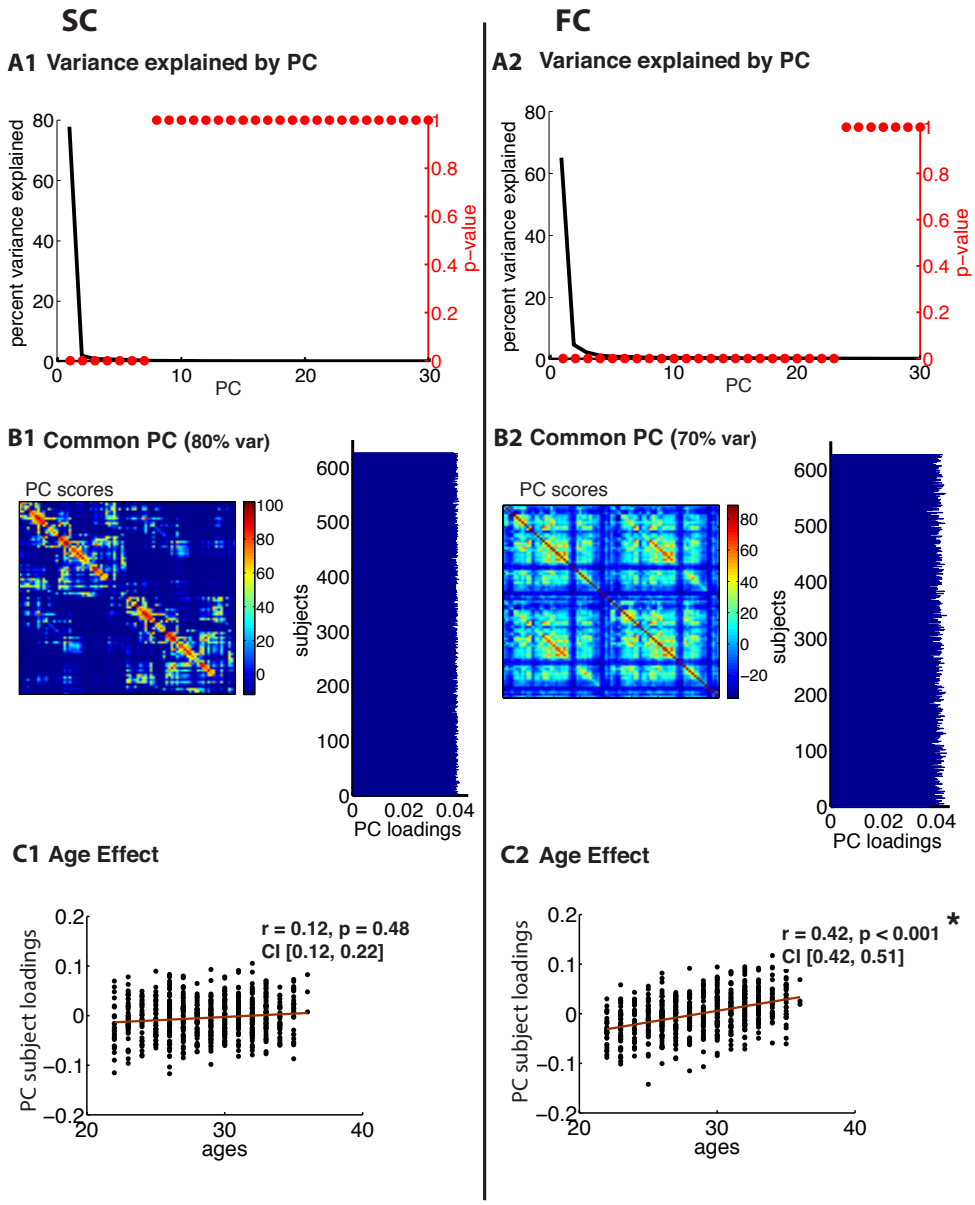

Figure 4. PCA of SC and FC matrices over all subjects of HCP Lausanne dataset. Percent of total variance explained by each principal component of the **A1)** SC and **A2)** FC, with corresponding p-values. Panel B shows on the left-hand-side the principal component scores per

connection for PC1, **B1)** for the SC, and **B2)** for the FC. This shows the aspects of the connectome that are manifested in PC1, the common (across subjects) component. On the right-hand-side of panel B are the subject loadings onto PC1, all subjects load positively on this component. **C1)** shows the age effect for the SC and **C2)** shows the age effect for the FC.

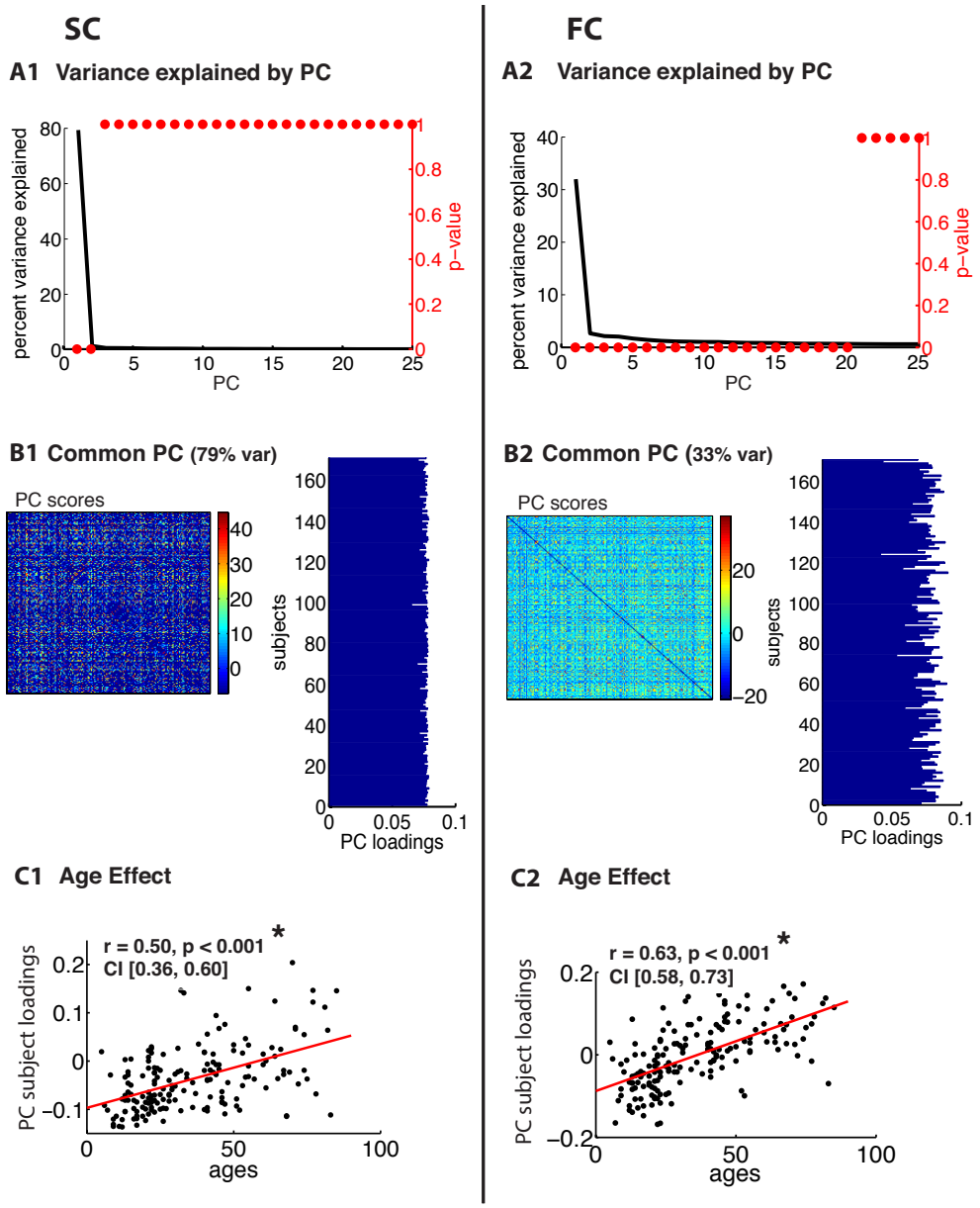

Figure 5. PCA of SC and FC matrices on Rockland dataset. Percent of total variance explained by each principal component of the **A1)** SC and **A2)** FC, with corresponding p-values. Panel B

shows on the left-hand-side the principal component scores per connection for PC1, **B1)** for the SC, and **B2)** for the FC. This shows the aspects of the connectome that are manifested in PC1, the common (across subjects) component. On the right-hand-side of panel B are the subject loadings onto PC1, all subjects load positively on this component. **C1)** shows the age effect for the SC and **C2)** shows the age effect for the FC.

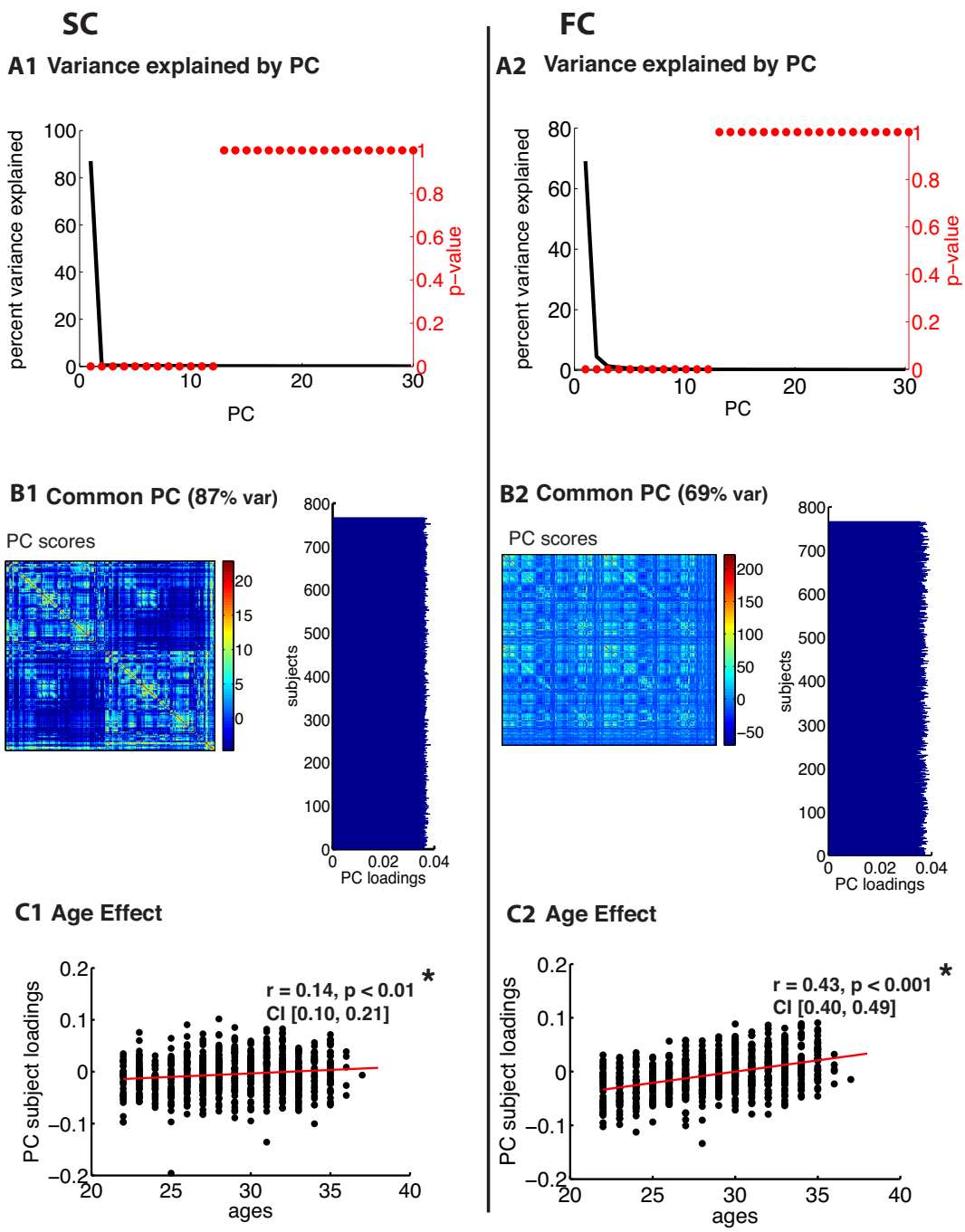

Figure 6. PCA of SC and FC matrices on HCP Glasser data. Percent of total variance explained by each principal component of the **A1)** SC and **A2)** FC, with corresponding p-values. Panel B shows on the left-hand-side the principal component scores per connection for PC1, **B1)** for the SC, and **B2)** for the FC. This shows the aspects of the connectome that are manifested in PC1, the common (across subjects) component. On the right-hand-side of panel B are the subject

loadings onto PC1, all subjects load positively on this component. **C1)** shows the age effect for the SC and **C2)** shows the age effect for the FC.

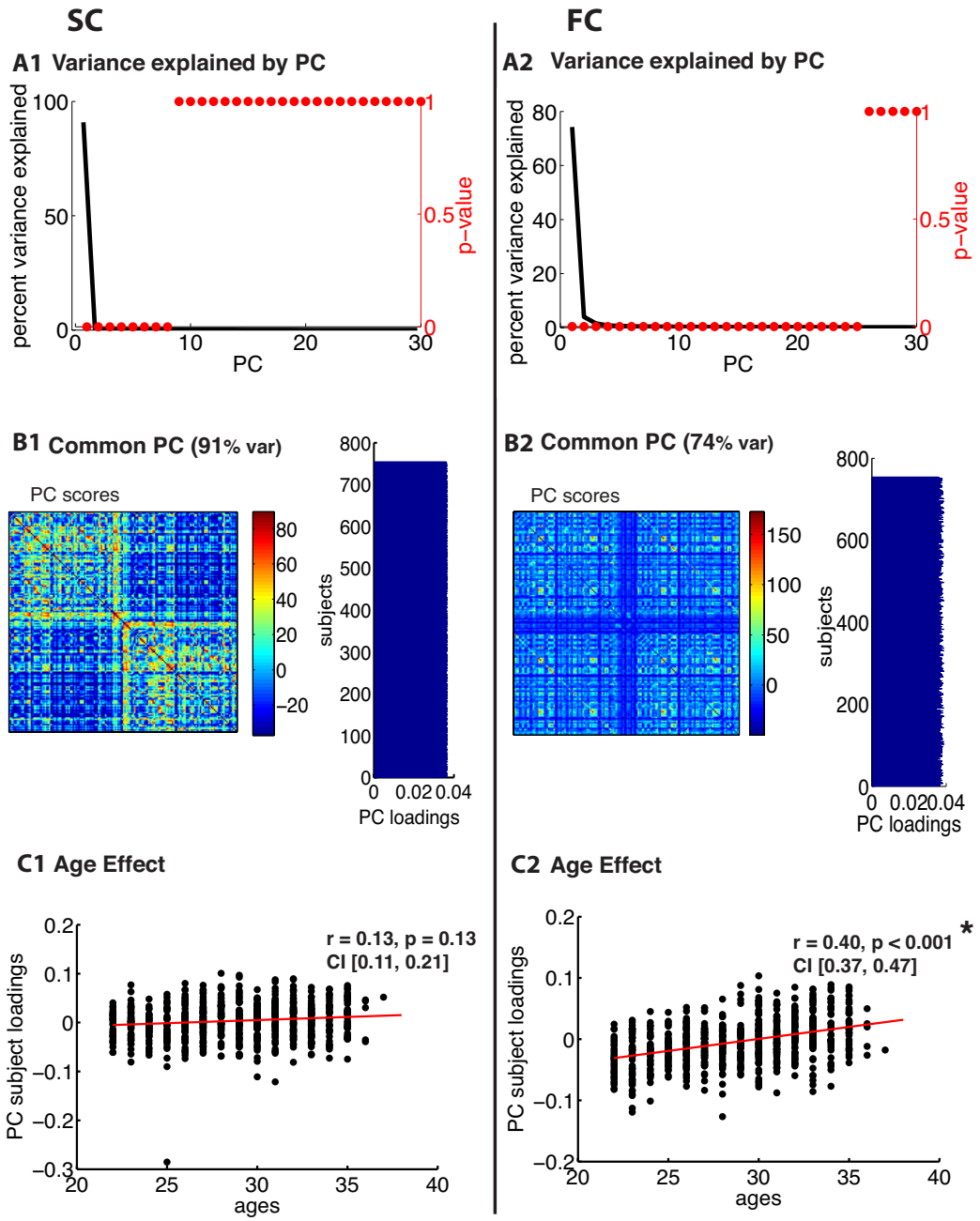

Figure 7. PCA of SC and FC matrices on HCP Destrieux data. Percent of total variance explained by each principal component of the **A1)** SC and **A2)** FC, with corresponding p-values. Panel B shows on the left-hand-side the principal component scores per connection for PC1, **B1)**

for the SC, and **B2)** for the FC. This shows the aspects of the connectome that are manifested in PC1, the common (across subjects) component. On the right-hand-side of panel B are the subject loadings onto PC1, all subjects load positively on this component. **C1)** shows the age effect for the SC and **C2)** shows the age effect for the FC.

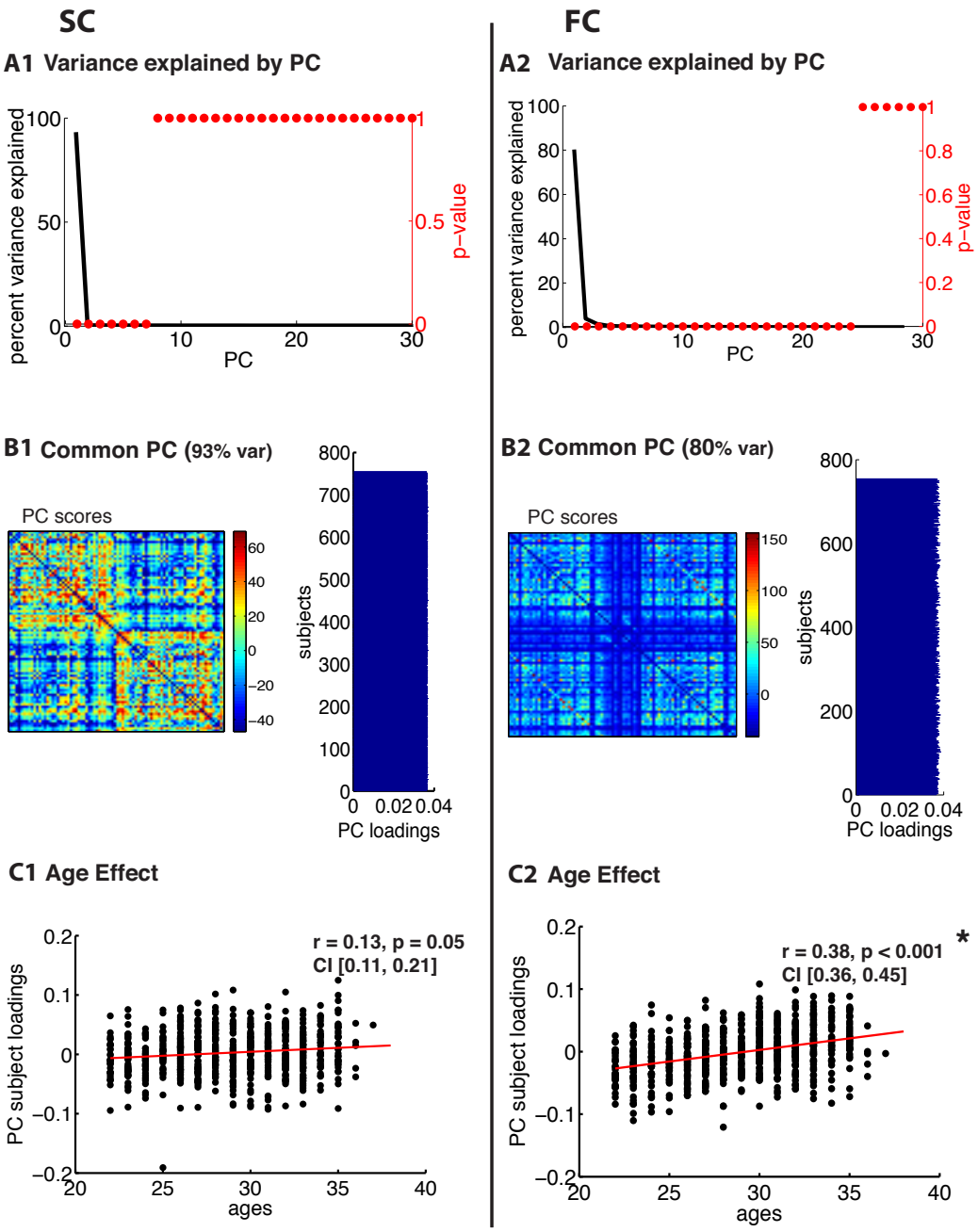

Figure 8. PCA of SC and FC matrices on HCP DK data. Percent of total variance explained by each principal component of the **A1)** SC and **A2)** FC, with corresponding p-values. Panel B shows on the left-hand-side the principal component scores per connection for PC1, **B1)** for the SC, and **B2)** for the FC. This shows the aspects of the connectome that are manifested in PC1, the common (across subjects) component. On the right-hand-side of panel B are the subject

loadings onto PC1, all subjects load positively on this component. **C1)** shows the age effect for the SC and **C2)** shows the age effect for the FC.

Discussion

Subject specificity in SC-FC

Initial studies of SC-FC correspondence (Greicius et al., 2009; Honey et al., 2007; Honey et al., 2009; Koch et al., 2002), show that there is a relationship between these two entities via linear (Honey et al., 2009) as well as other more complex methods (Misic et al., 2016). However, there remains a gap in our understanding of how the two measures relate at the individual level. In the present study, we showcase how individual SC corresponds with individual FC, using simple linear metrics in three separate datasets (Berlin, HCP, NKI Rockland) with variable acquisition, processing methods as well as age spectrums. The question was whether the correspondence of individual SC-FC matrices was greater than if two matrices were randomly paired.

Our results showed that although there is a correlation between group-averaged SC and FC, replicating previous findings (Greicius et al., 2009; Hermundstad et al., 2013; Honey et al., 2007; Honey et al., 2009; Koch et al., 2002; Misic et al., 2016; Ponce-Alvarez et al., 2015; Skudlarski et al., 2008; van den Heuvel et al., 2009), the specificity of this SC-FC relationship was not unique to an individual. Five of the datasets examined did not show subject specificity of the SC-FC correspondence, so that within-subject SC-FC did not exceed random pairings of SC-FC. This would suggest that individual SC cannot predict individual FC beyond chance. However, when the analysis was conducted on the HCP data with the Glasser parcellation, significant subject-specificity was observed. This would suggest that while subject-specificity assessed on

standard datasets via standard parcellation and processing methods is difficult to ascertain, it may be obvious only when higher resolution data *as well as* finer parcellations are applied.

Our finding that intra-subject SC-FC correspondence exceeded inter-subject SC-FC correspondence for the HCP Glasser dataset, but not for the HCP Lausanne, Berlin, or NKI Rockland dataset, supports the hypothesis by Honey et al. (2009), who speculated that the individual SC-FC fit would be significant if shown on a large enough dataset of high fidelity, which was demonstrated in the results from the Glasser-parcellated HCP dataset. Our interpretation is that this difference was due to the higher precision (Glasser) versus more standard (Lausanne) parcellation used. However, these two HCP datasets also differed in the tractography method (probabilistic vs deterministic). Thus we endeavoured to re-evaluate our findings post-hoc using two additional HCP datasets with probabilistic tractography processed in the same way as the Glasser HCP, except with finer grained parcellation methods, FreeSurfer convolution-based probabilistic Destrieux atlas (Destrieux et al., 2010) and Desikan-Killiany (DK) atlas (Desikan et al., 2006). We did not find subject-specificity with the HCP Destrieux and the HCP DK, suggesting that the Glasser parcellation allows for a fitting of individual structure and function that could not otherwise be observed. The Glasser multi-modal parcellation is based on functional properties with improved areal feature-based cross-subject alignment rather than solely geometric and morphological properties, and thus improves the neuroanatomical precision of individual parcellations. It is important to point out the despite the improvement, the Glasser HCP dataset was only slightly better than the others, and would not pass a direct head-to-head comparison since the presence of significance in one dataset and the absence of significance in another does not mean the two datasets are themselves significantly different.

Subject specificity in SC-FC is limited by variability within modality

The second set of findings clarify the unique portion of variance that exists in either modality alone, which may set limitations on the portion of SC that can reasonably be captured by individual FC. We had speculated that the lack of subject-specificity in the Berlin, HCP Lausanne and NKI Rockland dataset was due to a large portion of common variance in the connectomes across subjects that over-powered any existing individual differences. Indeed, our results conferred that there is a large portion of common variance in SC across subjects, however this was true regardless of the sample size, data quality, or parcellation: Berlin: 91%, HCP Lausanne: 80%, NKI: 79%, HCP Glasser: 87%, HCP Destrieux: 91%, HCP DK: 93%. Interestingly, even in the Glasser dataset, where whole-connectome SC-FC subject-specificity was observed, this component was strikingly large. We did observe, however, that SC variability was captured via a greater *number* of components in the Glasser dataset compared to the other datasets (Glasser N = 12, Berlin = 1, HCP Lausanne = 7, NKI Rockland = 2, HCP Destrieux = 8, HCP DK = 7), suggesting greater inter-individual differences in the SC. Although the smaller datasets (e.g. Berlin) generally had fewer SC components, the variability in the Glasser HCP SC was not merely due to sample size as the HCP Destrieux and HCP DK datasets were comparable in the number of subjects.

We also found that FC showed a large common component, which accounted for less total variance than the SC common component. Here, a larger number of significant components were observed. The comparably greater FC variability can be observed in the striping in the SC-FC correspondence matrix, where some FCs correlate quite highly with all SCs, while others

correlate very little with all SCs. Note that this does not mean that individual differences in SC are not observed, but rather that the correspondance of SC variance that maps to the corresponding variance in FC is weaker than one may expect intuitively.

In the FC, a significant portion of variance was related to age, particularly for the two datasets with a wide age range (Berlin, NKI: age = 20-80, 5-85). This is consistent with previous reports of age effects on FC (Andrews-Hanna et al., 2007; Damoiseaux et al., 2007; Ferreira & Busatto, 2013; Sala-Llonch et al., 2014)). Interestingly, however, age did not account for a significant portion of between-subject variance in SC for two (HCP Lausanne, Berlin) of the four datasets. In the third dataset (NKI Rockland), the large observed age effect in SC was likely a consequence of the wide age distribution and the inclusion of child subjects. The grey-white matter boundary is ill defined in children, and incomplete myelination results in weaker tractography-based estimation of SC (Deoni, Dean, Remer, Dirks, & O'Muircheartaigh, 2015; Thompson et al., 2005).

The limited amount of between-subjects variability in both SC and FC found in our study was comparable to Marellec et al (2016), where a large portion of variance was accounted for by an ‘invariant core’ (SC: ~86%, FC: ~59%). Here it was found that the invariant core of SC correlated with the invariant core of FC. Along the same lines, Waller et al. (2017) suggested that the specificity of connectome fingerprinting using FC was limited by the large amount of common variance across subjects.

The decomposition approach we used here is helpful for separating common and unique variance and identifying aspects of the connectome that express each portion of variance. Data-driven classification algorithms like clustering are an alternate approach that can be used to express similarities and differences between subject connectomes (E. Amico et al., 2017; Iraji et al., 2016) . Recently, a consensus clustering algorithm has been introduced that can be helpful for identifying how aspects of the connectome are combined to express these inter-subject similarities and differences (Rasero, 2017).

Limitations on the study of variability within modality

The study of variability within SC and FC each faces its unique limitations. Variation in acquisition, processing and connectome metrics and statistical methods may impact the extent of between-subject variability observed. For instance, for SC, the diffusion method, or tractography (Bonilha et al., 2015), SC metric (Buchanan, Pernet, Gorgolewski, Storkey, & Bastin, 2014), and ROI size (Bonilha et al., 2015), may affect variability and reproducibility of SCs. FC variability will similarly be affected by choice of metric. For example, the amount of common variance may be slightly higher using correlation compared to mutual information for the calculation of FC, whereas dynamic FC calculated over several smaller time windows shows a similar common 'invariant core' component across subjects as when FC was calculated over a single timeseries (Marrelec et al., 2016). In that study, parcellation or preprocessing did not have a large effect on FC variance.

The correlation between SC and FC may be limited by the dynamic fluctuation of FC on short time windows (Allen et al., 2014; Deco, Kringelbach, Jirsa, & Ritter, 2016; Hutchison et al.,

2013). SCs may better correlate with temporally stable rsFC (Honey et al., 2009). To this end, we considered only SC present connections in a secondary analysis, as these have been shown to have more stable resting-state FC (Shen et al., 2015).

One important question is whether increased between-subjects' variation in the FC is a consequence of non-neural influences such as vascular variability or head motion (Geerligs, Tsvetanov, Cam, & Henson, 2017) or reflects real, meaningful variability in neural activation. If meaningless between-subjects variability in FC can be reduced, FC has the best chance to be able to capture subtle individual differences in SC. In addition to the corrections described in the methods, FC between-subjects variability was minimized via a secondary global signal regression (GSR) analysis (Berlin dataset, NKI Rockland dataset). Yet, lack of SC-FC subject-specific correlation in five of the six persists despite these secondary analyses.

Future directions

Computational models that investigate how SC gives rise to FC may be particularly helpful for furthering our understanding of how individual SC and FC are linked (Ritter et al., 2013). The mechanisms by which individual FC comes about from individual SC may be the key to understanding subject-specific differences. In this sense, parameters from such generative models that are optimized based on the individual SC foundation and fitted to the empirical FC may be particularly revealing (Schirner, McIntosh, Jirsa, Deco, & Ritter, 2018). Variability in these parameters have already been shown to be relevant to brain function and behaviour in health (Jirsa, Sporns, Breakspear, Deco, & McIntosh, 2010; Kringelbach, McIntosh, Ritter, Jirsa, & Deco, 2015; Kunze, Hunold, Haueisen, Jirsa, & Spiegler, 2016; Roy et al., 2014) and disease

(Falcon, Jirsa, & Solodkin, 2016; Falcon, Riley, et al., 2016; Falcon et al., 2015; Jirsa et al., 2017; Jirsa et al., 2010).

Summary

We present evidence that the subject variation in SC, as estimated from diffusion weighted MRI, may be too weak in healthy populations to be reflected in the FC variability in most standard datasets. However, subject specificity of SC-FC can be captured via fine, multi-modally parcellated data, due to greater SC variability across subjects. Nonetheless, SC and FC each show a large component that is common across subjects which sets limitations on the extent of SC-FC subject specificity. Implications of these findings for personalized medicine should be considered. Namely, attention to the quality of processing and parcellation methods is critical for furthering our understanding of the relationship between individual SC and FC.

Acknowledgments

Data were provided [in part] by the Human Connectome Project, WU-Minn Consortium (Principal Investigators: David Van Essen and Kamil Ugurbil; 1U54MH091657) funded by the 16 NIH Institutes and Centers that support the NIH Blueprint for Neuroscience Research; and by the McDonnell Center for Systems Neuroscience at Washington University.

The authors gratefully acknowledge the computing time granted by the John von Neumann Institute for Computing (NIC) and provided on the supercomputer JURECA at Jülich Supercomputing Centre (JSC) (www.fz-juelich.de, Grant NIC#8344 & NIC#10276 to P.R.). The authors acknowledge the support of the NSERC grant (RGPIN-2017-06793) to A.R.M., and funding granted by the German Ministry of Education and Research (US-German Collaboration in Computational Neuroscience 01GQ1504A, Bernstein Focus State Dependencies of Learning 01GQ0971-5), the European Union Horizon2020 (ERC Consolidator Grant BrainModes 683049), Stiftung Charité/Private Exzellenzinitiative Johanna Quandt and Berlin Instititute of Health (BIH Johanna Quandt Professorship for Brain Simulation) to P.R.

References

Allen, E. A., Damaraju, E., Plis, S. M., Erhardt, E. B., Eichele, T., & Calhoun, V. D. (2014). Tracking whole-brain connectivity dynamics in the resting state. *Cereb Cortex, 24*(3), 663-676. doi:10.1093/cercor/bhs352

Amico, E., Goñi, J. (2017). The quest for identifiability in human functional connectomes. doi:arXiv:1707.02365

Amico, E., Marinazzo, D., Di Perri, C., Heine, L., Annen, J., Martial, C., . . . Goni, J. (2017). Mapping the functional connectome traits of levels of consciousness. *Neuroimage, 148*, 201-211. doi:10.1016/j.neuroimage.2017.01.020

Andrews-Hanna, J. R., Snyder, A. Z., Vincent, J. L., Lustig, C., Head, D., Raichle, M. E., & Buckner, R. L. (2007). Disruption of large-scale brain systems in advanced aging. *Neuron, 56*(5), 924-935. doi:10.1016/j.neuron.2007.10.038

Bonilha, L., Gleichgerrcht, E., Fridriksson, J., Rorden, C., Breedlove, J. L., Nesland, T., . . . Focke, N. K. (2015). Reproducibility of the Structural Brain Connectome Derived from Diffusion Tensor Imaging. *PLoS One, 10*(8), e0135247. doi:10.1371/journal.pone.0135247

Brown, J. A., Rudie, J. D., Bandrowski, A., Van Horn, J. D., & Bookheimer, S. Y. (2012). The UCLA multimodal connectivity database: a web-based platform for brain connectivity matrix sharing and analysis. *Front Neuroinform, 6*, 28. doi:10.3389/fninf.2012.00028

Buchanan, C. R., Pernet, C. R., Gorgolewski, K. J., Storkey, A. J., & Bastin, M. E. (2014). Test-retest reliability of structural brain networks from diffusion MRI. *Neuroimage, 86*, 231-243. doi:10.1016/j.neuroimage.2013.09.054

Caeyenberghs, K., Leemans, A., Leunissen, I., Michiels, K., & Swinnen, S. P. (2013). Topological correlations of structural and functional networks in patients with traumatic brain injury. *Front Hum Neurosci, 7*, 726. doi:10.3389/fnhum.2013.00726

Cattell, R. B. (1966). The Scree Test For The Number Of Factors. *Multivariate Behavioral Research, 1*(2), 245-276. doi:10.1207/s15327906mbr0102_10

Cocchi, L., Harding, I. H., Lord, A., Pantelis, C., Yucel, M., & Zalesky, A. (2014). Disruption of structure-function coupling in the schizophrenia connectome. *Neuroimage Clin, 4*, 779-787. doi:10.1016/j.nicl.2014.05.004

Damoiseaux, J. S., Beckmann, C. F., Arigita, E. J., Barkhof, F., Scheltens, P., Stam, C. J., . . . Rombouts, S. A. (2007). Reduced resting-state brain activity in the "default network" in normal aging. *Cereb Cortex*.

Deco, G., Kringelbach, M. L., Jirsa, V., & Ritter, P. (2016). The dynamics of resting fluctuations in the brain: metastability and its dynamical cortical core. *bioRxiv*. doi:10.1101/065284

Deoni, S. C., Dean, D. C., 3rd, Remer, J., Dirks, H., & O'Muircheartaigh, J. (2015). Cortical maturation and myelination in healthy toddlers and young children. *Neuroimage, 115*, 147-161. doi:10.1016/j.neuroimage.2015.04.058

Desikan, R. S., Segonne, F., Fischl, B., Quinn, B. T., Dickerson, B. C., Blacker, D., . . . Killiany, R. J. (2006). An automated labeling system for subdividing the human cerebral cortex on MRI scans into gyral based regions of interest. *Neuroimage, 31*(3), 968-980. doi:10.1016/j.neuroimage.2006.01.021

Destrieux, C., Fischl, B., Dale, A., & Halgren, E. (2010). Automatic parcellation of human cortical gyri and sulci using standard anatomical nomenclature. *Neuroimage, 53*(1), 1-15. doi:10.1016/j.neuroimage.2010.06.010

Enrico, A., Goñi, J. The quest for identifiability in human functional connectomes. *arXiv*. doi: arXiv:1707.02365

Falcon, M. I., Jirsa, V., & Solodkin, A. (2016). A new neuroinformatics approach to personalized medicine in neurology: The Virtual Brain. *Curr Opin Neurol, 29*(4), 429-436. doi:10.1097/WCO.0000000000000344

Falcon, M. I., Riley, J. D., Jirsa, V., McIntosh, A. R., Chen, E. E., & Solodkin, A. (2016). Functional Mechanisms of Recovery after Chronic Stroke: Modeling with the Virtual Brain. *eNeuro, 3*(2). doi:10.1523/ENEURO.0158-15.2016

Falcon, M. I., Riley, J. D., Jirsa, V., McIntosh, A. R., Shereen, A. D., Chen, E. E., & Solodkin, A. (2015). The Virtual Brain: Modeling Biological Correlates of Recovery after Chronic Stroke. *Front Neurol, 6*, 228. doi:10.3389/fneur.2015.00228

Ferreira, L. K., & Busatto, G. F. (2013). Resting-state functional connectivity in normal brain aging. *Neurosci Biobehav Rev, 37*(3), 384-400. doi:10.1016/j.neubiorev.2013.01.017

Finn, E. S., Shen, X., Scheinost, D., Rosenberg, M. D., Huang, J., Chun, M. M., . . . Constable, R. T. (2015). Functional connectome fingerprinting: identifying individuals using patterns of brain connectivity. *Nat Neurosci, 18*(11), 1664-1671. doi:10.1038/nn.4135

Geerligs, L., Tsvetanov, K. A., Cam, C., & Henson, R. N. (2017). Challenges in measuring individual differences in functional connectivity using fMRI: The case of healthy aging. *Hum Brain Mapp, 38*(8), 4125-4156. doi:10.1002/hbm.23653

Glasser, M. F., Coalson, T. S., Robinson, E. C., Hacker, C. D., Harwell, J., Yacoub, E., . . . Van Essen, D. C. (2016). A multi-modal parcellation of human cerebral cortex. *Nature, 536*(7615), 171-178. doi:10.1038/nature18933

Glasser, M. F., Sotiropoulos, S. N., Wilson, J. A., Coalson, T. S., Fischl, B., Andersson, J. L., . . . Consortium, W. U.-M. H. (2013). The minimal preprocessing pipelines for the Human Connectome Project. *Neuroimage, 80*, 105-124. doi:10.1016/j.neuroimage.2013.04.127

Greicius, M. D., Supekar, K., Menon, V., & Dougherty, R. F. (2009). Resting-State Functional Connectivity Reflects Structural Connectivity in the Default Mode Network. *Cereb Cortex, 19*(1), 72-78. doi:10.1093/cercor/bhn059

Hagmann, P., Cammoun, L., Gigandet, X., Meuli, R., Honey, C. J., Wedeen, V., & Sporns, O. (2008). Mapping the structural core of human cerebral cortex. *Plos Biology, 6*(7), 1479-1493. doi:e159

10.1371/journal.pbio.0060159

Hearne, L. J., Mattingley, J. B., & Cocchi, L. (2016). Functional brain networks related to individual differences in human intelligence at rest. *Sci Rep, 6*, 32328. doi:10.1038/srep32328

Hermundstad, A. M., Bassett, D. S., Brown, K. S., Aminoff, E. M., Clewett, D., Freeman, S., . . . Carlson, J. M. (2013). Structural foundations of resting-state and task-based functional connectivity in the human brain. *Proc Natl Acad Sci U S A, 110*(15), 6169-6174. doi:10.1073/pnas.1219562110

Honey, C. J., Kotter, R., Breakspear, M., & Sporns, O. (2007). Network structure of cerebral cortex shapes functional connectivity on multiple time scales. *Proc Natl Acad Sci U S A, 104*(24), 10240-10245.

Honey, C. J., Sporns, O., Cammoun, L., Gigandet, X., Thiran, J. P., Meuli, R., & Hagmann, P. (2009). Predicting human resting-state functional connectivity from structural connectivity. *Proc Natl Acad Sci U S A, 106*(6), 2035-2040. doi:0811168106 [pii]

10.1073/pnas.0811168106

Hutchison, R. M., Womelsdorf, T., Allen, E. A., Bandettini, P. A., Calhoun, V. D., Corbetta, M., . . . Chang, C. (2013). Dynamic functional connectivity: promise, issues, and interpretations. *Neuroimage, 80*, 360-378. doi:10.1016/j.neuroimage.2013.05.079

Iraji, A., Calhoun, V. D., Wiseman, N. M., Davoodi-Bojd, E., Avanaki, M. R. N., Haacke, E. M., & Kou, Z. (2016). The connectivity domain: Analyzing resting state fMRI data using feature-based data-driven and model-based methods. *Neuroimage, 134*, 494-507. doi:10.1016/j.neuroimage.2016.04.006

Jirsa, V. K., Proix, T., Perdikis, D., Woodman, M. M., Wang, H., Gonzalez-Martinez, J., . . . Bartolomei, F. (2017). The Virtual Epileptic Patient: Individualized whole-brain models of epilepsy spread. *Neuroimage, 145*(Pt B), 377-388. doi:10.1016/j.neuroimage.2016.04.049

Jirsa, V. K., Sporns, O., Breakspear, M., Deco, G., & McIntosh, A. R. (2010). Towards the virtual brain: network modeling of the intact and the damaged brain. *Arch Ital Biol, 148*(3), 189-205.

Jülich Supercomputing Centre. (2016). JURECA: General-purpose supercomputer at Jülich Supercomputing Centre. Journal of large-scale research facilities, 2, A62. doi:10.17815/jlsrf-2-121

Koch, M. A., Norris, D. G., & Hund-Georgiadis, M. (2002). An investigation of functional and anatomical connectivity using magnetic resonance imaging. *Neuroimage, 16*(1), 241-250. doi:10.1006/nimg.2001.1052

S1053811901910523 [pii]

Kringelbach, M. L., McIntosh, A. R., Ritter, P., Jirsa, V. K., & Deco, G. (2015). The Rediscovery of Slowness: Exploring the Timing of Cognition. *Trends Cogn Sci, 19*(10), 616-628. doi:10.1016/j.tics.2015.07.011

Krishnan, A., Williams, L. J., McIntosh, A. R., & Abdi, H. (2011). Partial Least Squares (PLS) methods for neuroimaging: a tutorial and review. *Neuroimage, 56*(2), 455-475. doi:10.1016/j.neuroimage.2010.07.034

Kumar, K., Desrosiers, C., Siddiqi, K., Colliot, O., & Toews, M. (2017). Fiberprint: A subject fingerprint based on sparse code pooling for white matter fiber analysis. *Neuroimage, 158*, 242-259. doi:10.1016/j.neuroimage.2017.06.083

Kunze, T., Hunold, A., Haueisen, J., Jirsa, V., & Spiegler, A. (2016). Transcranial direct current stimulation changes resting state functional connectivity: A large-scale brain network modeling study. *Neuroimage, 140*, 174-187. doi:10.1016/j.neuroimage.2016.02.015

Markett, S., Weber, B., Voigt, G., Montag, C., Felten, A., Elger, C., & Reuter, M. (2013). Intrinsic connectivity networks and personality: the temperament dimension harm avoidance moderates functional connectivity in the resting brain. *Neuroscience, 240*, 98-105. doi:10.1016/j.neuroscience.2013.02.056

Marrelec, G., Messe, A., Giron, A., & Rudrauf, D. (2016). Functional Connectivity's Degenerate View of Brain Computation. *PLoS Comput Biol, 12*(10), e1005031. doi:10.1371/journal.pcbi.1005031

McIntosh, A. R., & Lobaugh, N. J. (2004). Partial least squares analysis of neuroimaging data: applications and advances. *Neuroimage, 23 Suppl 1*, S250-263.

Meier, J., Tewarie, P., Hillebrand, A., Douw, L., van Dijk, B. W., Stufflebeam, S. M., & Van Mieghem, P. (2016). A Mapping Between Structural and Functional Brain Networks. *Brain Connect, 6*(4), 298-311. doi:10.1089/brain.2015.0408

Misic, B., Betzel, R. F., de Reus, M. A., van den Heuvel, M. P., Berman, M. G., McIntosh, A. R., & Sporns, O. (2016). Network-Level Structure-Function Relationships in Human Neocortex. *Cereb Cortex, 26*(7), 3285-3296. doi:10.1093/cercor/bhw089

Munsell, B. C., Hofesmann, E., Delgaizo, J., Styner, M., Bonilha, L. . (2017). Identifying Subnetwork Fingerprints in Structural Connectomes: A Data-Driven Approach. *International Workshop on Connectomics in Neuroimaging*. doi:https://link.springer.com/chapter/10.1007/978-3-319-67159-8_10

Ponce-Alvarez, A., Deco, G., Hagmann, P., Romani, G. L., Mantini, D., & Corbetta, M. (2015). Resting-state temporal synchronization networks emerge from connectivity topology and heterogeneity. *PLoS Comput Biol, 11*(2), e1004100. doi:10.1371/journal.pcbi.1004100

Ponsoda, V., Martinez, K., Pineda-Pardo, J. A., Abad, F. J., Olea, J., Roman, F. J., . . . Colom, R. (2017). Structural brain connectivity and cognitive ability differences: A multivariate distance matrix regression analysis. *Hum Brain Mapp, 38*(2), 803-816. doi:10.1002/hbm.23419

Rasero, J., Pellicoro, M., Angelini, L., Cortes, J.M., Marinazzo, D., Stramaglia, S. (2017). Consensus clustering approach to group brain connectivity matrices. *Network Neuroscience, 1*(3), 242-253. doi:https://doi.org/10.1162/netn_a_00017

Ritter, P., Schirner, M., McIntosh, A. R., & Jirsa, V. K. (2013). The virtual brain integrates computational modeling and multimodal neuroimaging. *Brain Connect, 3*(2), 121-145. doi:10.1089/brain.2012.0120

Romero-Garcia, R., Atienza, M., & Cantero, J. L. (2014). Predictors of coupling between structural and functional cortical networks in normal aging. *Hum Brain Mapp, 35*(6), 2724-2740. doi:10.1002/hbm.22362

Roy, D., Sigala, R., Breakspear, M., McIntosh, A. R., Jirsa, V. K., Deco, G., & Ritter, P. (2014). Using the virtual brain to reveal the role of oscillations and plasticity in shaping brain's dynamical landscape. *Brain Connect, 4*(10), 791-811. doi:10.1089/brain.2014.0252

Sala-Llonch, R., Junque, C., Arenaza-Urquijo, E. M., Vidal-Pineiro, D., Valls-Pedret, C., Palacios, E. M., . . . Bartres-Faz, D. (2014). Changes in whole-brain functional networks and memory performance in aging. *Neurobiol Aging, 35*(10), 2193-2202. doi:10.1016/j.neurobiolaging.2014.04.007

Schirner, M., McIntosh, A. R., Jirsa, V., Deco, G., & Ritter, P. (2018). Inferring multi-scale neural mechanisms with brain network modelling. *Elife, 7*. doi:10.7554/eLife.28927

Schirner, M., Rothmeier, S., Jirsa, V. K., McIntosh, A. R., & Ritter, P. (2015). An automated pipeline for constructing personalized virtual brains from multimodal neuroimaging data. *Neuroimage, 117*, 343-357. doi:10.1016/j.neuroimage.2015.03.055

Shen, K., Misic, B., Cipollini, B. N., Bezgin, G., Buschkuehl, M., Hutchison, R. M., . . . Berman, M. G. (2015). Stable long-range interhemispheric coordination is supported by direct anatomical projections. *Proc Natl Acad Sci U S A, 112*(20), 6473-6478. doi:10.1073/pnas.1503436112

Skudlarski, P., Jagannathan, K., Anderson, K., Stevens, M. C., Calhoun, V. D., Skudlarska, B. A., & Pearlson, G. (2010). Brain connectivity is not only lower but different in schizophrenia: a combined anatomical and functional approach. *Biol Psychiatry, 68*(1), 61-69. doi:10.1016/j.biopsych.2010.03.035

Skudlarski, P., Jagannathan, K., Calhoun, V. D., Hampson, M., Skudlarska, B. A., & Pearlson, G. (2008). Measuring brain connectivity: diffusion tensor imaging validates resting state temporal correlations. *Neuroimage, 43*(3), 554-561. doi:10.1016/j.neuroimage.2008.07.063

Smith, S. (2016). Linking cognition to brain connectivity. *Nat Neurosci, 19*(1), 7-9. doi:10.1038/nn.4206

Smith, S. M., Nichols, T. E., Vidaurre, D., Winkler, A. M., Behrens, T. E., Glasser, M. F., . . . Miller, K. L. (2015). A positive-negative mode of population covariation links brain connectivity, demographics and behavior. *Nat Neurosci, 18*(11), 1565-1567. doi:10.1038/nn.4125

Thompson, P. M., Sowell, E. R., Gogtay, N., Giedd, J. N., Vidal, C. N., Hayashi, K. M., . . . Toga, A. W. (2005). Structural MRI and brain development. *Int Rev Neurobiol, 67*, 285-323. doi:10.1016/S0074-7742(05)67009-2

van den Heuvel, M. P., Mandl, R. C., Kahn, R. S., & Hulshoff Pol, H. E. (2009). Functionally linked resting-state networks reflect the underlying structural connectivity architecture of the human brain. *Hum Brain Mapp, 30*(10), 3127-3141. doi:10.1002/hbm.20737

van den Heuvel, M. P., & Sporns, O. (2013). An anatomical substrate for integration among functional networks in human cortex. *J Neurosci, 33*(36), 14489-14500. doi:10.1523/JNEUROSCI.2128-13.2013

Van Essen, D. C., Smith, S. M., Barch, D. M., Behrens, T. E., Yacoub, E., Ugurbil, K., & Consortium, W. U.-M. H. (2013). The WU-Minn Human Connectome Project: an overview. *Neuroimage, 80*, 62-79. doi:10.1016/j.neuroimage.2013.05.041

Waller, L., Walter, H., Kruschwitz, J. D., Reuter, L., Muller, S., Erk, S., & Veer, I. M. (2017). Evaluating the replicability, specificity, and generalizability of connectome fingerprints. *Neuroimage, 158*, 371-377. doi:10.1016/j.neuroimage.2017.07.016

Yeh, F. C., Vettel, J. M., Singh, A., Poczos, B., Grafton, S. T., Erickson, K. I., . . . Verstynen, T. D. (2016). Quantifying Differences and Similarities in Whole-Brain White Matter Architecture Using Local Connectome Fingerprints. *PLoS Comput Biol, 12*(11), e1005203. doi:10.1371/journal.pcbi.1005203

Zhang, Z., Liao, W., Chen, H., Mantini, D., Ding, J. R., Xu, Q., . . . Lu, G. (2011). Altered functional-structural coupling of large-scale brain networks in idiopathic generalized epilepsy. *Brain, 134*(Pt 10), 2912-2928. doi:10.1093/brain/awr223

Zimmermann, J., Ritter, P., Shen, K., Rothmeier, S., Schirner, M., & McIntosh, A. R. (2016). Structural architecture supports functional organization in the human aging brain at a regionwise and network level. *Hum Brain Mapp, 37*(7), 2645-2661. doi:10.1002/hbm.23200